Earth and Planetary Science Letters 359-360 (2012) 194–205

Contents lists available at SciVerse ScienceDirect

Earth and Planetary Science Letters

journal homepage: www.elsevier.com/locate/epsl

Re–Os geochronology of the lacustrine Green River Formation: Insights into direct depositional dating of lacustrine successions, Re–Os systematics and paleocontinental weathering

Vivien M. Cumming [a,*], David Selby [a], Paul G. Lillis [b]

[a] Department of Earth Sciences, Durham University, Durham, DH1 3LE, UK
[b] US Geological Survey, Box 25046, MS977, Denver Federal Centre, Denver, CO 80225, USA

ARTICLE INFO

Article history:
Received 16 May 2012
Received in revised form
26 September 2012
Accepted 11 October 2012
Editor: T. Elliot
Available online 16 November 2012

Keywords:
Re–Os geochronology
lacustrine
Green River Formation
Uinta basin
osmium

ABSTRACT

Lacustrine sedimentary successions provide exceptionally high-resolution records of continental geological processes, responding to tectonic, climatic and magmatic influences. These successions are therefore essential for correlating geological and climatic phenomena across continents and furthermore the globe. Producing accurate geochronological frameworks within lacustrine strata is challenging because the stratigraphy is often bereft of biostratigraphy and directly dateable tuff horizons. The rhenium–osmium (Re–Os) geochronometer is a well-established tool for determining precise and accurate depositional ages of marine organic-rich rocks. Lake systems with stratified water columns are predisposed to the preservation of organic-rich rocks and thus should permit direct Re–Os geochronology of lacustrine strata. We present Re–Os systematics from one of the world's best documented lacustrine systems, the Eocene Green River Formation, providing accurate Re–Os depositional dates that are supported by Ar–Ar and U–Pb ages of intercalated tuff horizons. Precision of the Green River Formation Re–Os dates is controlled by the variation in initial $^{187}Os/^{188}Os$ and the range of $^{187}Re/^{188}Os$ ratios, as also documented in marine systems. Controls on uptake and fractionation of Re and Os are considered to relate mainly to depositional setting and the type of organic matter deposited, with the need to further understand the chelating precursors of Re and Os in organic matter highlighted. In addition to geochronology, the Re–Os data records the $^{187}Os/^{188}Os$ composition of lake water (1.41–1.54) at the time of deposition, giving an insight into continental runoff derived from weathering of the geological hinterland of the Green River Formation. Such insights enable us to evaluate fluctuations in continental climatic, tectonic and magmatic processes and provide the ability for chemostratigraphic correlation combined with direct depositional dates. Furthermore, initial $^{187}Os/^{188}Os$ values can be used as a diagnostic tool to distinguish between lacustrine and marine depositional settings when compared to known oceanic $^{187}Os/^{188}Os$ values.

1. Introduction

Lake systems are common to the continental landscape throughout the world and frequently record deposition over millions of years (e.g., Carroll et al., 1992; Olsen, 1997). Lacustrine sediments provide a valuable archive of continental geological processes, at a much higher resolution than globally averaged marine records (Pietras and Carroll, 2006). The importance of lacustrine deposits is exemplified by the numerous studies providing vital insights into processes such as continental tectonics and magmatism, paleoclimatic fluctuations, geomagnetic timescales, Milankovitch cycles, terrestrial biotic evolution and economic resources (e.g., Carroll and Bohacs, 1999; Hao et al., 2011; Katz, 2001; Lambiase, 1990; Machlus et al., 2004; Meyers, 2008). Sedimentation in lake settings can range from fluvial to highly organic-rich profundal deposits documenting a complex amalgamation of continental and atmospheric processes. A more complete understanding of the relationship of lacustrine sediments to global geological systems requires accurate and precise geochronological frameworks. Age control in lacustrine settings is often hampered by the lack of biostratigraphic constraints common to the marine record. In the absence of tuff horizons for U–Pb and Ar–Ar geochronology, or sufficient and documented mammalian biostratigraphy, direct dating of lacustrine sedimentary stratigraphy is challenging.

The Re–Os geochronometer is a widely-used tool for determining precise and accurate depositional ages of marine organic-rich rocks (e.g., Cohen et al., 1999; Georgiev et al., 2011;

* Corresponding author. Tel.: +44 191 3342300; fax: +44 191 3342301.
E-mail address: v.m.cumming@durham.ac.uk (V.M. Cumming).

0012-821X/$ - see front matter © 2012 Elsevier B.V. All rights reserved.
http://dx.doi.org/10.1016/j.epsl.2012.10.012

Kendall et al., 2009a; Selby and Creaser, 2005; Xu et al., 2009). These and additional studies have demonstrated that Re–Os systematics are not adversely affected by processes such as hydrocarbon maturation and greenschist-grade metamorphism (e.g., Creaser et al., 2002; Kendall et al., 2004; Rooney et al., 2012, 2010; Yang et al., 2009). However, application of the Re–Os geochronometer to lacustrine strata has only been partially evaluated (Creaser et al., 2008; Poirier and Hillaire-Marcel, 2011). Here we present a comprehensive study of one of the world's best documented lacustrine systems, the Green River Formation (GRF), to assess whether Re–Os geochronology can be used as a tool to directly date the deposition of lacustrine organic-rich rocks.

Previous studies suggest the uptake of Re and Os in marine organic-rich rocks relies on the capture of hydrogenous Re and Os at or below the sediment/water interface under oxygen limited conditions (Cohen et al., 1999; Colodner et al., 1993; Crusius et al., 1996; Ravizza and Turekian, 1992; Ravizza et al., 1991), with the majority of Re and Os bound in organic matter (Cohen et al., 1999; Georgiev et al., 2011; Rooney et al., 2012; Selby and Creaser, 2003). This implies that organic-rich rocks deposited in reducing bottom waters of a stratified lake should be predisposed to Re and Os uptake, and thus viable for Re–Os geochronology, provided there is sufficient runoff containing dissolved Re and Os. As interpreted for the marine realm, the initial $^{187}Os/^{188}Os$ (Os_i) composition of lacustrine organic-rich rocks should reflect the $^{187}Os/^{188}Os$ composition of lake water at the time of deposition (Cohen et al., 1999; Ravizza and Turekian, 1992, 1989). The $^{187}Os/^{188}Os$ composition of seawater records a balance of radiogenic ($\sim$1.40) continental inputs derived chiefly from runoff with minor contributions from aeolian dust, and unradiogenic ($\sim$0.12) inputs derived from cosmic dust and hydrothermal alteration of oceanic crust (Peucker-Ehrenbrink and Ravizza, 2000). Assuming that runoff from the surrounding continental crust is the predominant source of Os into a lake, the $^{187}Os/^{188}Os$ composition of lake water will reflect the composition of regional continental runoff at the time of deposition. Os isotopes therefore provide an insight into regional geological processes and allow chemostratigraphic correlation making Re–Os geochronology beneficial beyond direct depositional age dating.

Here we evaluate and discuss lacustrine Re–Os geochronology and Os isotope compositions of the GRF in the Uinta Basin, Utah, USA. The GRF succession represents a classic model of lacustrine sediment deposition and is primarily comprised of organic-rich carbonaceous siltstones, mudstones and marly oil shales (Keighley et al., 2003; Smith et al., 2008a; Tuttle and Goldhaber, 1993). Interbedded tuff horizon Ar–Ar and U–Pb dates provide an extensive geochronological framework, which has been tied to mammalian biostratigraphy, paleomagnetic and astronomical ages (Smith et al., 2010, 2008a, 2006, 2003). This temporal framework makes the GRF an ideal natural laboratory for testing the applicability of the Re–Os geochronometer to lacustrine deposits.

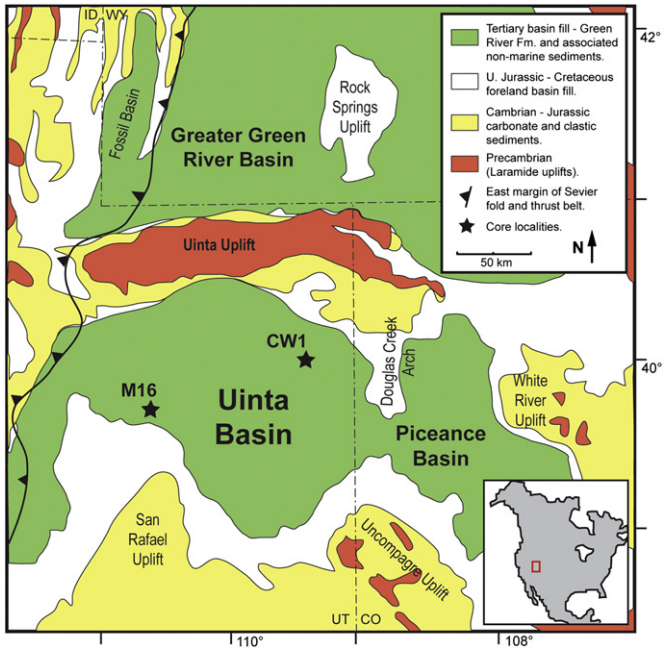

Fig. 1. Location map displaying the main basins containing the Green River Formation, the surrounding geology and the location of the sampled Marsing 16 (M16; 39°57′ 1.4904″N, 111°1′37.527″W) and Coyote Wash 1 (CW1; 40°1′22.224″N, 109°18′38.4834″W) cores in the Uinta Basin (adapted from Smith et al., 2008a). The GRF basins formed east of the thin-skinned Sevier orogenic belt, and are separated by Laramide basement-cored uplifts, the geometry of which is controlled by Precambrian and late Palaeozoic structures (Johnson, 1992). These structures were occupied by two large lakes covering an area of 65,000 km^2 during the early to middle Eocene. The CW1 core is located in the central depocentre of an asymmetric basin structure (See Fig. 2, inset A), while the M16 core is proximal to the lake margin. Inset map of North America shows the study area.

2. Geological setting

2.1. Geology of the Green River Formation basins

The GRF was deposited in three main continental basins (Fig. 1: Uinta, Piceance and Greater Green River), in Colorado, Wyoming and Utah (Dyni, 2006). The extensive Green River lake system was associated with temperate to subtropical climate of the early to middle Eocene (Smith et al., 2008a), which resulted in exceptionally high continental denudation rates (175 ± 30 m/Myr; Smith et al., 2008b). Sedimentary facies within the GRF can be divided into fluvio-lacustrine, fluctuating profundal and evaporative facies (Carroll and Bohacs, 1999, 2001; Fig. 2). Deposition occurred in freshwater to hypersaline lakes with lake-level fluctuations resulting in thick packages of organic-rich carbonaceous shales interbedded with fluvial clastic deposits (Keighley et al., 2003; Pietras and Carroll, 2006). The final stages of GRF deposition occurred at the end of the Laramide orogeny when the basins were infilled from the north by volcanics from the Absaroka volcanic field (Johnson, 1992). The Uinta Basin was the final basin to be infilled and therefore had the longest-lived lake containing the thickest section of GRF (>3 km). Organic-rich units from the Uinta basin were sampled for this study as they record the complete history of the GRF.

2.2. Uinta Basin stratigraphy

Lacustrine deposition in the Uinta Basin began in the early Eocene following eastward retreat of the Late Cretaceous seaway (Ryder et al., 1976). Initial deposition began with the Colton Formation (coarse grained clastic beds and red mudstones), which was deposited in a fluvial setting. As lake-levels rose the depositional setting evolved into fluvio-lacustrine deposition of sandstones interbedded with the base of the GRF and at the lake edges (Fig. 2). Stratigraphically above the Colton Formation, the Douglas Creek Member of the GRF was deposited in response to rising lake-levels (Bradley, 1931; Tuttle and Goldhaber, 1993). The Douglas Creek Member is a siliciclastic-dominated interval with fluvial sandstones and siltstones deposited at the edges of the basin and oil shales deposited in the central depocentres, considered correlative to the green shale and black shale facies of the GRF in other parts of the basin (Remy, 1992; Ruble et al., 2001). This depositional model has been attributed to fluctuating profundal facies deposition (Carroll and Bohacs, 2001). Following deposition of this interval an increase in salinity is

attributed to the development of a more arid climate between 49 and 50 Ma (Ryder et al., 1976; Tuttle and Goldhaber, 1993). Increased aridity resulted in evaporitic deposition of saline minerals interbedded with dolomitic marlstones, mudstones, sandstones and oil shales of the carbonate dominated Parachute Creek Member, stratigraphically above the Douglas Creek Member (Fig. 2). The basal section of the Parachute Creek Member (~49 Ma) records a rise in lake-levels to their maximum extent that resulted in the deposition of oil shales interbedded with mudstones, marlstones and siltstones. This section, the Mahogany Zone, is the most organic-rich horizon of the GRF (total organic carbon [TOC] up to 30 wt%; Bradley, 1931; Smith et al., 2008a; Tuttle and Goldhaber, 1993). Deposition in the Uinta Basin continued until ~44 Ma with conditions becoming progressively more evaporitic (Smith et al., 2008a). Above the Parachute Creek Member red-brown shale and fluvial coarse-grained clastics make up interbeds of the Uinta Formation of the GRF (Keighley et al., 2003).

2.3. Previous geochronology

The current geochronological framework for the GRF is based on Ar–Ar ages of interbedded tuffs concentrated in the Greater Green River and Uinta Basins (Smith et al., 2008a; 2006; 2003). More recently, the Ar–Ar ages have been recalibrated to Fish Canyon Sanidine (KO_8) and accurately correlated to U–Pb zircon ages from the tuff beds and astronomical ages preserved within cyclical sediments (Kuiper et al., 2008; Smith et al., 2010). Uinta Basin deposition began ~52 Ma, but the oldest dated tuff is the Curly tuff at 49.32 ± 0.30 Ma lying just below the Mahogany Zone (Fig. 2). This makes correlation of the older stratigraphy in the Uinta Basin more difficult, especially as there is a lack of surface exposure (Smith et al., 2008a). Lacustrine deposition ended just after deposition of the Strawberry tuff dated at 44.27 ± 0.93 Ma. Geochronology in the Uinta Basin allows cross-correlation of Re–Os and Ar–Ar ages in order to assess the accuracy of Re–Os lacustrine organic-rich rock geochronology.

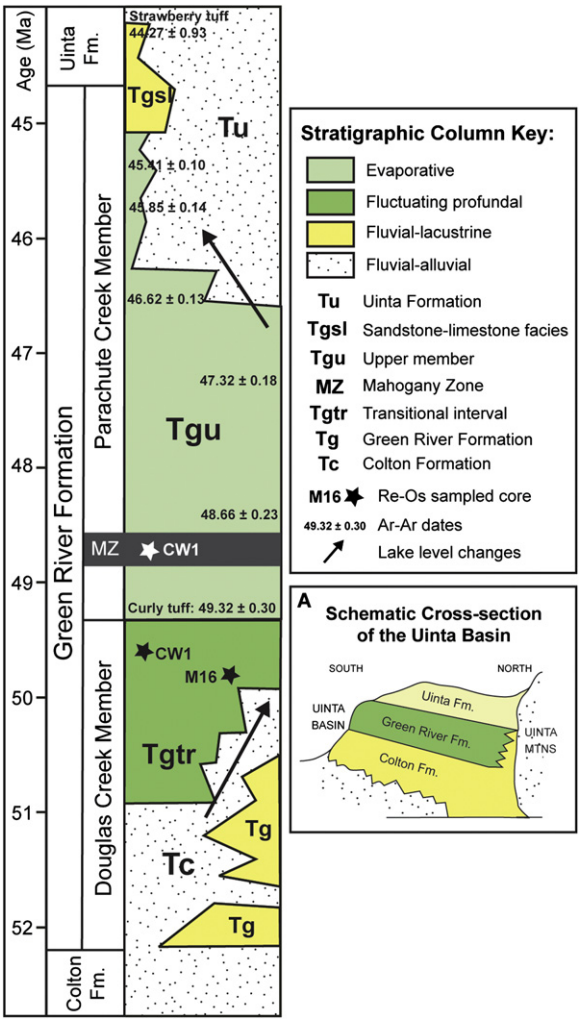

Fig. 2. Generalised chronostratigraphy displaying the main members of the GRF and the location of sampled units. Age constraints labelled on the stratigraphic column are based on Ar–Ar dates of interbedded tuffs. Lacustrine facies associations of each unit are illustrated in the right hand panel of the stratigraphic column; these are adapted from lithostratigraphy of Smith et al. (2008a). This lithostratigraphy illustrates the complex nature of spatial and temporal variation of units within the Uinta basin. Nomenclature of Smith et al. (2008a) is included in the key in order to aid comparison with Ar–Ar ages. Inset A is a simplified cross-section of the Uinta Basin at the present day that illustrates the asymmetric nature of the basin and that the erosional remnant now outcrops within the southern limb of a gentle syncline, dipping $< 5^{\circ}$ to the North. The southern margin of the basin has mostly been eroded, with the most continuous exposure in the northeast corner of the basin where up to ~4 km of sediment was deposited. With a lack of surface exposure this asymmetric nature makes correlation of units challenging.

3. Sampling and methodology

Uinta Basin GRF samples were collected from two exploration drill-cores (Coyote Wash 1 [CW1] and Marsing 16 [M16]; Fig. 1). The Mahogany Zone and the Douglas Creek Member were sampled as these are the most organic-rich intervals of GRF in the Uinta Basin (3.5–28.1 wt% TOC: Table 1). The sampled stratigraphy comprises grey–black carbonaceous mudstones and oil shales of the profundal dominated intervals. All sampled core sections are absent of alteration and veining. Re–Os isotope analysis was performed at Durham University's TOTAL laboratory for source rock geochronology and geochemistry following published methods used for Re–Os dating of marine organic-rich rocks (Selby, 2007; Selby and Creaser, 2003). TOC analysis and Rock-Eval pyrolysis was performed at Weatherford labs, Houston. A detailed description of the samples and methods used for this study is provided in the Supplementary Material.

4. Results

4.1. TOC and Rock-Eval

The TOC and Rock-Eval pyrolysis results for all samples are presented in Table 1. The Douglas Creek Member (M16) has the lowest TOC of the 3 sections (3.5 to 9.7 wt%), with the Douglas Creek Member (CW1) possessing highly variable TOC (2.6 to 24.7 wt%), with 9 of the 12 samples yielding TOC < 10 wt%. In comparison, the Mahogany Zone (CW1) possesses TOC values between 9.3 and 28.1 wt%, with 9 of 11 samples analysed yielding TOC > 10 wt%. Rock-Eval pyrolysis is used to assess the type and maturity of organic matter in the samples. The T_{max} (assessment of maturity using the temperature at maximum generation of remaining hydrocarbons after free oil is removed) values for all the samples are similar and range between 432 and 448 °C signifying moderate maturity. The type of organic matter in our samples is assessed using the hydrogen and oxygen indexes (HI versus OI), as screening proxies to the van Krevelen atomic H/C versus O/C diagram (Espitalie et al., 1977; Peters, 1986; Fig. 3). The HI and OI data illustrate that all samples are Type I kerogen, consistent with previous GRF studies (Katz, 1995; Tissot et al., 1978).

4.2. Re–Os geochronology

The Re and Os abundances for the Douglas Creek Member (M16) are 21.0–62.4 ppb and 178–490 ppt, respectively (Table 1). This is a substantial enrichment in comparison to estimates for average continental crust (0.2–1 ppb Re and 30–50 ppt Os; Esser and Turekian, 1993; Hattori et al., 2003; Peucker-Ehrenbrink and Jahn, 2001; Sun et al., 2003). These abundances generally co-vary and are comparable to abundances in marine organic-rich rocks (e.g., Cohen et al., 1999; Kendall et al., 2009a; Selby and Creaser, 2005; Xu et al., 2009). The $^{187}Re/^{188}Os$ and $^{187}Os/^{188}Os$ ratios range from 328.6 to 1015.2 and 1.82 to 2.35, respectively. Linear regression of the Re–Os data yields a Model 3 age of 48.4 ± 2.7 Ma (2σ, n=13, Mean Squared of Weighted Deviation [MSWD]=6.8, Os_i=1.54 ± 0.03; Fig. 4A; all ages include ^{187}Re decay constant uncertainty). Douglas Creek Member samples (CW1) are also enriched in Re and Os with abundances of 10.5–83.5 ppb and 114–412 ppt, respectively (Table 1). The $^{187}Re/^{188}Os$ ratios range from 326.9 to 1830.5, with $^{187}Os/^{188}Os$ ratios between 1.57 and 2.89. Linear regression of the Re–Os data yields a Model 3 age of 49.8 ± 4.8 Ma (2σ, n=13, MSWD=39, Os_i=1.41 ± 0.06; Fig. 4D). Samples from the Mahogany Zone (CW1) also display enriched Re and Os abundances ranging from 11.8 to 39.5 ppb and 198 to 815 ppt, respectively (Table 1). The $^{187}Re/^{188}Os$ values have a limited range from 296 to 451 but exhibit a positive correlation to the $^{187}Os/^{188}Os$ values ranging from 1.72 to 1.83. Regression of this Re-Os data yields a Model 1 age of 47.8 ± 9.9 Ma (2σ, n=13, MSWD=0.43, Os_i of 1.48 ± 0.06; Fig. 4F).

Table 1
Re–Os isotope data, total organic carbon (TOC) content and Rock-Eval data for the Green River Formation samples.

Sample	Depth (m)	Re (ppb)	±	Os (ppt)	±	^{192}Os (ppt)	±	$^{187}Re/^{188}Os$	±	$^{187}Os/^{188}Os$	±	rho [a]	Os_i [b]	TOC (wt%)	T_{max} [c] (°C)	S1 [d]	S2 [e]	S3 [f]	HI [g]	OI [h]
Douglas Creek Member, Marsing 16 core (39°57′1.4904″N, 111°1′37.527″W)																				
M16-27[i]	323.8	22.6	0.1	341.3	2.3	115.3	0.9	390.2	3.3	1.831	0.018	0.722	1.52	5.96	435	2.33	59.28	0.81	994	13.6
M16-26[i]	323.9	23.6	0.1	333.5	2.6	112.3	1.0	418.3	4.1	1.861	0.022	0.718	1.52	6.47	437	2.17	51.46	0.74	796	11.4
M16-25[i]	324.0	42.6	0.1	490.0	2.8	163.4	0.9	518.6	3.3	1.950	0.013	0.680	1.53	9.71	437	2.89	68.68	0.86	707	8.9
M16-24[i]	324.0	27.8	0.1	393.8	3.0	132.7	1.2	417.4	4.0	1.854	0.022	0.704	1.52	7.09	440	2.85	54.60	0.78	770	11.0
M16-23[i]	324.5	54.9	0.2	341.6	1.9	109.5	0.6	997.4	6.5	2.336	0.014	0.819	1.53	8.20	435	1.99	61.77	0.93	753	11.3
M16-22[i]	324.6	56.0	0.2	343.1	2.1	109.8	0.7	1015.2	7.1	2.352	0.016	0.790	1.53	–	–	–	–	–	–	–
M16-21[i]	324.6	62.4	0.2	392.8	2.5	126.0	0.8	984.8	6.9	2.326	0.017	0.735	1.53	5.42	438	1.91	44.93	0.69	829	12.7
M16-20[i]	324.7	40.1	0.1	351.6	1.5	115.7	0.4	690.2	3.2	2.079	0.008	0.599	1.52	5.53	441	2.10	49.53	0.73	896	13.2
M16-19[i]	324.7	24.5	0.1	263.1	1.4	87.5	0.4	556.4	3.4	1.982	0.013	0.665	1.53	3.53	437	1.64	33.23	0.78	942	22.1
M16-18[j]	324.9	29.2	0.1	273.4	1.5	90.0	0.4	645.0	3.8	2.078	0.013	0.651	1.56	6.39	448	2.23	68.53	0.89	1073	13.9
M16-16[j]	325.1	21.0	0.1	178.2	1.2	58.2	0.4	716.3	5.5	2.145	0.019	0.725	1.57	5.71	443	13.44	51.69	0.81	906	14.2
M16-15[j]	325.3	22.9	0.1	297.1	1.6	99.4	0.5	458.1	2.7	1.923	0.012	0.648	1.55	5.23	442	1.56	42.36	0.73	811	14.0
M16-14[j]	325.4	16.8	0.1	300.2	1.8	101.5	0.6	328.6	2.2	1.819	0.014	0.654	1.55	4.87	445	1.23	42.67	0.75	877	15.4
Douglas Creek Member, Coyote Wash 1 core (40°1′22.224″N, 109°18′38.4834″W)																				
CW1-40[k]	1026.0	23.4	0.1	307.8	1.7	104.6	0.6	445.0	2.9	1.774	0.012	0.682	1.40	6.01	441	2.13	52.15	1.59	867	26.4
CW1-41[k]	1026.1	14.6	0.1	258.5	1.9	89.0	0.8	326.9	3.2	1.654	0.020	0.699	1.38	7.55	444	1.72	63.99	1.90	848	25.2
CW1-42[k]	1026.2	10.5	0.0	184.0	1.5	63.3	0.7	330.0	3.6	1.657	0.022	0.732	1.38	6.83	442	2.35	57.89	1.95	847	28.5
CW1-44	1026.5	14.2	0.1	245.4	1.8	85.2	0.8	331.7	3.3	1.573	0.020	0.702	1.30	7.07	442	1.50	73.03	1.24	1032	17.5
CW1-45	1026.6	30.3	0.1	256.7	1.5	84.9	0.5	711.0	4.7	2.028	0.014	0.728	1.44	9.98	439	5.24	106.70	1.28	1069	12.8
CW1-46	1026.8	34.9	0.1	303.2	1.6	100.2	0.5	692.4	4.2	2.036	0.013	0.695	1.46	7.44	438	3.06	76.44	1.06	1027	14.2
CW1-48[k]	1027.0	15.3	0.1	145.4	1.3	48.6	0.6	627.6	7.4	1.921	0.027	0.756	1.40	2.67	434	2.62	22.24	1.03	832	38.5
CW1-49[k]	1027.2	83.5	0.3	298.9	1.8	90.7	0.5	1830.5	11.1	2.889	0.018	0.712	1.37	7.85	441	2.74	83.74	0.92	1066	11.7
CW1-50[k]	1027.4	46.6	0.2	412.1	3.8	137.3	1.5	675.1	7.6	1.963	0.032	0.635	1.40	15.46	440	4.48	146.19	1.20	946	7.8
CW1-51	1027.5	11.5	0.0	114.3	1.1	38.2	0.5	600.3	8.2	1.936	0.030	0.807	1.44	4.97	436	1.22	42.69	0.86	859	17.3
CW1-53	1027.7	17.7	0.1	180.5	1.4	60.2	0.6	584.4	5.9	1.960	0.023	0.751	1.47	–	–	–	–	–	–	–
CW1-54[k]	1027.8	39.1	0.1	346.0	1.9	115.3	0.6	674.9	4.1	1.956	0.013	0.645	1.40	24.70	438	8.12	222.95	1.51	903	6.1
CW1-55	1028.0	33.8	0.1	385.3	2.1	129.5	0.7	519.5	3.1	1.879	0.012	0.635	1.45	16.92	437	5.05	163.78	1.30	968	7.7
Mahogany Zone, Coyote Wash 1 core (40°1′22.224″N, 109°18′38.4834″W)																				
CW1-05	682.5	15.2	0.1	294.0	2.3	100.5	1.0	301.1	3.2	1.716	0.022	0.719	1.48	11.28	439	6.45	117.31	2.13	1040	18.9
CW1-06	682.7	28.0	0.1	486.0	2.9	165.7	1.0	336.0	2.4	1.746	0.014	0.673	1.48	22.78	443	11.69	237.11	1.92	1041	8.4
CW1–07	682.8	25.5	0.1	464.1	2.8	158.5	1.0	320.2	2.3	1.730	0.014	0.673	1.48	22.59	445	9.55	248.16	2.10	1099	9.3
CW1–09	683.2	26.7	0.1	362.6	4.5	122.6	2.2	433.0	7.8	1.822	0.048	0.668	1.48	25.82	436	11.95	272.55	1.81	1055	7.0
CW1–10	683.4	20.8	0.1	383.2	3.0	130.8	1.2	316.4	3.2	1.735	0.022	0.698	1.48	14.47	437	7.47	149.11	2.04	1031	14.1
CW1–12	683.6	15.5	0.1	264.2	2.8	89.9	1.4	344.1	5.3	1.765	0.036	0.721	1.49	9.69	434	6.65	95.36	2.48	985	25.6
CW1–13	683.7	15.6	0.1	295.3	2.4	100.8	1.0	307.1	3.4	1.737	0.023	0.717	1.49	9.39	434	6.84	96.77	2.01	1031	21.4
CW1–14	683.9	16.7	0.1	326.8	3.3	111.8	1.6	297.9	4.5	1.717	0.034	0.710	1.48	–	–	–	–	–	–	–
CW1–15	684.3	11.8	0.0	198.4	2.2	67.5	1.1	349.0	5.8	1.768	0.037	0.742	1.49	10.30	439	6.29	108.94	2.20	1058	21.4
CW1–16	684.5	14.6	0.1	286.2	2.3	97.7	1.0	296.6	3.3	1.730	0.024	0.717	1.49	11.35	441	5.70	119.94	1.68	1057	14.8
CW1–20	684.9	32.7	0.1	426.9	5.3	144.1	2.7	451.2	8.5	1.837	0.048	0.684	1.48	28.15	436	13.85	265.66	1.80	944	6.4
CW1–22	685.2	39.2	0.1	559.9	4.4	189.4	1.6	411.3	3.8	1.816	0.023	0.612	1.49	21.14	432	10.45	223.98	2.01	1060	9.5
CW1–23	685.4	20.1	0.1	366.4	3.2	125.0	1.4	320.1	3.7	1.737	0.026	0.704	1.48	–	–	–	–	–	–	–

All uncertainties are stated at 2σ.

[a] Rho is the associated error correlation at 2σ (Ludwig, 1980).
[b] Os_i is the initial $^{187}Os/^{188}Os$ isotope ratio calculated at 48.4, 49.8 and 47.8 Ma for each unit, respectively.
[c] T_{max}=temperature at maximum evolution of S2 hydrocarbons.
[d] S1=free oil content (mg hydrocarbons/g of rock).
[e] S2=remaining hydrocarbon potential (mg hydrocarbons/g of rock).
[f] S3=organic carbon dioxide (mg CO_2/g of rock).
[g] HI=Hydrogen Index (mg hydrocarbon/g C_{org}).
[h] OI=Oxygen Index (mg CO_2/g C_{org}).
[i] Re–Os Age=49.2 ± 1.0 Ma.
[j] Re–Os Age=50.1 ± 2.6 Ma.
[k] Re–Os Age=48.7 ± 0.6 Ma.

5. Discussion

5.1. Re–Os lacustrine organic-rich rock geochronology

Regression of all Re–Os data from the individually sampled sections of the CW1 and M16 cores yield ages that agree, within uncertainty, with the GRF Ar–Ar and U–Pb dates (see Section 5.2). However, Model 3 ages and large MSWD values strongly suggest that any scatter about the isochron is controlled by geological factors, rather than purely analytical uncertainties (Ludwig, 2008). Precise Re–Os geochronology requires samples with similar Os_i, and a spread in $^{187}Re/^{188}Os$ ratios of at least a few hundred units (Kendall et al., 2009a; Selby and Creaser, 2005). To assess whether samples have similar Os_i, the isotopic compositions of each sample are back-calculated using the ^{187}Re decay constant (1.666×10^{-11} a^{-1}; Smoliar et al., 1996) and the age determined from the respective isochron (Table 1).

Regression of the Douglas Creek Member (M16) yields a Model 3 age of 48.4 ± 2.7 Ma, (MSWD=6.8; Fig. 4A). The calculated Os_i at 48.4 Ma for all the samples varies from 1.52 to 1.57, with stratigraphically lower samples having higher Os_i values of 1.55–1.57 ($n=4$) and the remaining stratigraphically higher samples possessing Os_i values of 1.52–1.53 ($n=9$). Separate regression of the Re–Os data based on the Os_i values (1.55–1.57 and 1.52–1.53; Table 1), yield Model 1 ages of 50.1 ± 2.6 Ma (2σ, $n=4$, MSWD=0.43, $Os_i=1.54 \pm 0.02$; Fig. 4C) and 49.2 ± 1.0 Ma (2σ, $n=9$, MSWD=0.99, $Os_i=1.52 \pm 0.01$; Fig. 4B), respectively. Both of these ages are identical within uncertainty, with the 49.2 ± 1.0 Ma date providing the most precise depositional age for the Douglas Creek Member. The Model 1 ages and lower MSWD values suggest that stratigraphic changes in Os_i values is the principal control on the degree of scatter associated with the isochron of all M16 samples. The precise and accurate ages for these subsets strongly discounts any post-depositional disturbance to the Re–Os system. The stratigraphic variation in Os_i suggests a change in Os inputs or alteration of the balance and/or flux of Os inputs into the lake over time. In the case of the M16 samples, the 1 m of stratigraphy sampled could represent approximately 2.5–10 Ka (Smith et al., 2008a).

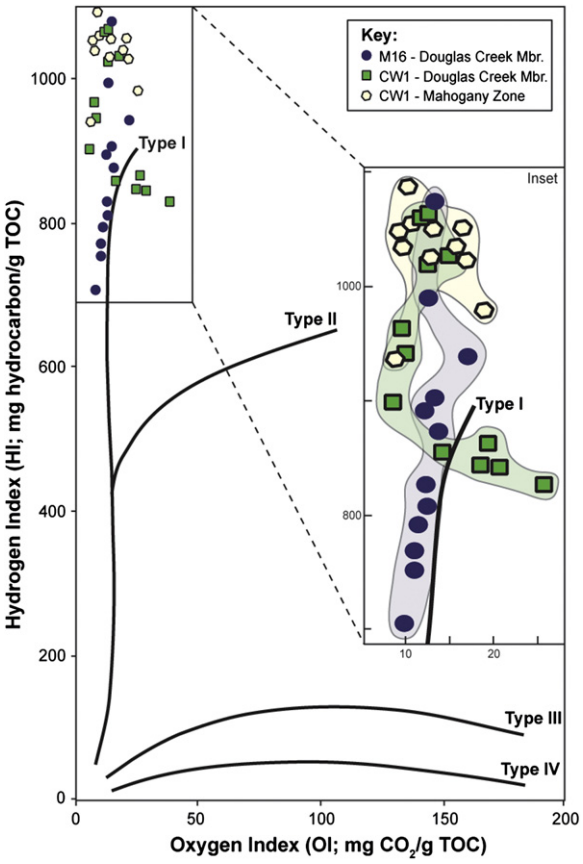

Fig. 3. Graph of hydrogen index versus oxygen index (HI/OI) as a proxy to an atomic H/C versus atomic O/C van Krevelen diagram (Espitalie et al., 1977; Peters, 1986). Lines for kerogen Types I to IV are annotated on the graph (taken from Hunt, 1996). All the samples are plotted illustrating that they are all Type I kerogen. The enlarged inset shows the area where samples are plotted with each of the sampled units outlined in order to demonstrate the variation in each horizon. See text for further discussion.

The Douglas Creek Member (CW1) yields a Model 3 age of 49.8 ± 4.8 Ma with an MSWD of 39 (Fig. 4D). The Os_i values calculated at 49.8 Ma vary substantially (1.30–1.47; Table 1). Unlike the Douglas Creek Member (M16), there is no stratigraphic relationship to Os_i in this core, suggesting that Os influx into the basin was very heterogeneous or that the Re–Os isotopic system has been disturbed during post-depositional processes. The isochronous nature of the samples and good agreement between the Re–Os data and Ar–Ar geochronology of the GRF suggest limited or no disturbance to the Re–Os system. We suggest that the scatter about the linear regression relates to variations in the Os_i of these samples (Fig. 4D inset). Interestingly seven of the samples have similar Os_i (1.37–1.40) and regression of this Re–Os data yields a precise Model 1 age of 48.7 ± 0.6 Ma (2σ, $n=7$, MSWD=1.8, $Os_i=1.41 \pm 0.01$; Table 1; Fig. 4E).

The Mahogany Zone (CW1) Re–Os data yield a Model 1 age of 47.8 ± 9.9 Ma, MSWD 0.43 (Fig. 4F). The Os_i values calculated at 47.8 Ma are very similar (1.48 to 1.49; Table 1) and $^{187}Re/^{188}Os$ and $^{187}Os/^{188}Os$ values display limited spread through this core (150 and 0.1 units, respectively). These ranges are much smaller than the Douglas Creek Member (M16 and CW1) sections which have ranges in $^{187}Re/^{188}Os$ values >650 and >1500 units, respectively and ranges in $^{187}Os/^{188}Os$ values >0.5 and >1.3 units, respectively. The lower MSWD is due to the very small range in $^{187}Os/^{188}Os$, which exaggerates the measured uncertainty thereby permitting an isochron fit. The larger uncertainty in the age for the Mahogany Zone CW1 can be attributed to the small ranges in $^{187}Os/^{188}Os$ and $^{187}Re/^{188}Os$. In an attempt to increase the variation in $^{187}Re/^{188}Os$ values, the sampled interval was increased from 2 m to 3 m (see Fig. 4), however $^{187}Re/^{188}Os$ and $^{187}Os/^{188}Os$ values remained extremely similar. The small spread cannot be attributed to sampling or analytical problems as the same protocols were used for all units and previous studies on marine sequences (e.g. Kendall et al., 2009a, Rooney et al., 2012; Selby and Creaser, 2005).

A limited spread in $^{187}Re/^{188}Os$ of organic-rich rocks has also been seen for marine units. For example, over the Frasnian–Famennian (F–F) boundary $^{187}Re/^{188}Os$ values range only ~20 units, with the Re–Os data yielding an imprecise date of 476 ± 140 Ma (Turgeon et al., 2007). Three other units surrounding the F–F boundary produced more precise ages with $^{187}Re/^{188}Os$ values spanning 200–400 units. The low spread in $^{187}Re/^{188}Os$ was interpreted to be the result of Re drawdown due to increasing anoxia (Turgeon et al., 2007), with the dated interval at the F–F boundary recording the highest sea-level and most anoxic stage compared to the other dated intervals (Johnson et al., 1985; Ver Straeten et al., 2011). Likewise, it has also been suggested that in restricted basins organic matter sedimentation draws down dissolved Re and Os from the water column thus shortening residence time and causing rapid variations in Os_i values due to higher sensitivity to changes in Os inputs (McArthur et al., 2008). This may be the case for the Douglas Creek Member (CW1) unit where we see the largest variation in Os_i values which is causing scatter about the isochron (Fig. 4D). However, large

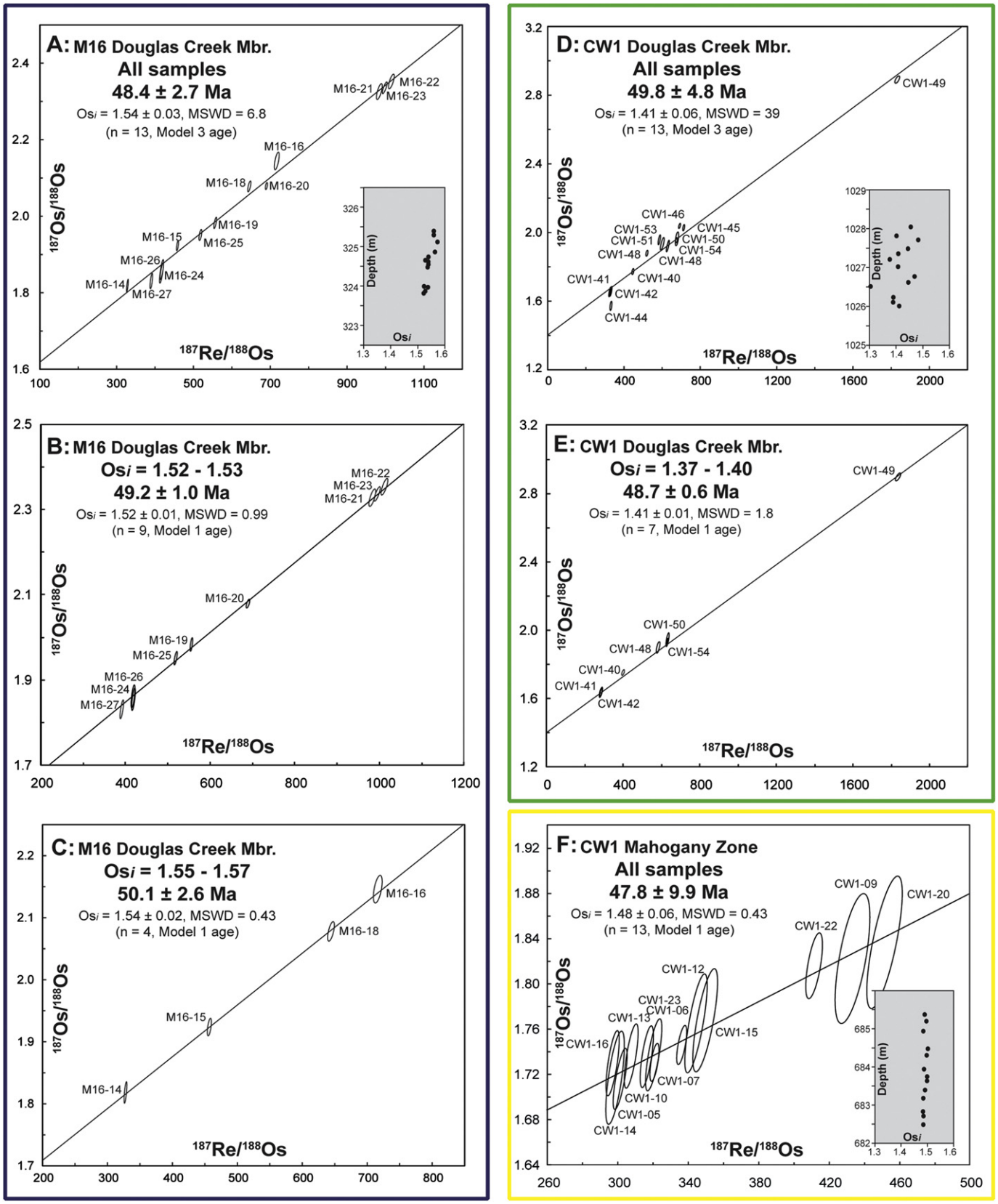

Fig. 4. Re–Os isochron diagrams for the Douglas Creek Member in the Marsing 16 core (A, B and C) and the Coyote Wash 1 core (D and E), and for the Mahogany Zone (F). The Re–Os isotopic data including the 2σ calculated uncertainties for $^{187}Re/^{188}Os$ and $^{187}Os/^{188}Os$ and the associated error correlation function (rho) are regressed to yield a Re–Os date using *Isoplot V.* 4.0 and the λ ^{187}Re constant of 1.666×10^{-11} a^{-1} (Ludwig, 2008, 1980; Smoliar et al., 1996). The age uncertainty including the uncertainty of 0.35% in the ^{187}Re decay constant (Selby et al., 2007; Smoliar et al., 1996) only affects the third decimal place. A Model 1 isochron is accomplished by assuming that scatter along the regression line is derived only from the input of 2σ uncertainties for $^{187}Re/^{188}Os$ and $^{187}Os/^{188}Os$, and ρ (rho). MSWD = Mean Squared of Weighted Deviation. Data point ellipses are 2σ uncertainties. Isochrons A, D and F represent regression of all the samples for each horizon and isochrons B, C and E represent regression of samples with similar initial $^{187}Os/^{188}Os$ (see text for discussion). Isochron E provides a precise depositional age for the Douglas Creek Member (CW1); however, although it agrees within uncertainty of the other ages, it has questionable validity due to the nature of the Os_i variation (see text for discussion). It can also be suggested that isochron E is pinned by sample CW1-49, but when the other 6 points are regressed they produce a Model 1 age of 51.0 ± 2.7 Ma (2σ, $n = 6$, MSWD = 1.5, $Os_i = 1.39 \pm 0.02$) which is within uncertainty of the seven point Re–Os seen in isochron E. The inset graphs show the Os_i versus depth of the samples for each horizon. The scales are the same for each graph so the variation in sampling depth and Os_i is visible. The sampled horizon for the Douglas Creek Member in the M16 core is 1.6 m, in the CW1 core it is 2 m and in the Mahogany Zone in the CW1 core it is 2.9 m.

gradients in Os_i values are not observed in the GRF and there is no significant change in Re and Os abundance through the sampled intervals suggesting that Re and Os drawdown does not occur. In similarity to the F–F boundary interval, the Mahogany Zone was deposited during the highest lake-levels and most anoxic period (Bradley, 1931; Tuttle and Goldhaber, 1993). We suggest that, rather than having intense Re or Os drawdown, the Mahogany Zone depositional environment (high lake-level, steady sedimentation and stable water column stratification; Smith et al., 2008a; Tuttle and Goldhaber, 1993) allowed for homogenous Re and Os uptake and thus minimal fractionation throughout the sampled interval, which hampers the utility of the strata for precise Re–Os geochronology.

In addition, it has been suggested that organic-rich rocks deposited in terrestrial basins will possess low $^{187}Re/^{188}Os$ values (<200; Baioumy et al., 2011). However, the $^{187}Re/^{188}Os$ data for all GRF sections is >200, with two of the sections (Douglas Creek Member) that represent more restricted deposition yielding significant variation in $^{187}Re/^{188}Os$ ratios (328–1831), similar to marine organic-rich rocks (Kendall et al., 2009a and references therein). As such, our findings contradict previous studies that suggest restricted and terrestrial deposits may not be viable for Re–Os geochronology (Baioumy et al., 2011; McArthur et al., 2008). We suggest that lacustrine deposits, like marine systems, vary enormously and basins should be assessed individually for Re–Os geochronology.

5.2. Comparison of Re–Os dates with Ar–Ar geochronology in the Uinta Basin

Although the Uinta Basin is an intensively studied lacustrine succession, correlation of the stratigraphy is hampered by informal and overlapping terminology, mainly due to a lack of surface exposure (Remy, 1992; Smith et al., 2008a). In this case Ar–Ar geochronology provides the ability to assess the accuracy of the Re–Os dates of the GRF lacustrine organic-rich rocks, although the Ar–Ar dates are more precise. The Curly tuff (Ar–Ar: 49.32 ± 0.30 Ma) is the oldest tuff dated in the Uinta Basin, lying $\sim$50 m below the Mahogany Zone at the top of the Transitional interval (Smith et al., 2008a). This interval forms part of the lower Parachute Creek Member and the upper Douglas Creek Member (Fig. 2), defined as a time of fluctuating profundal deposition (Smith et al., 2008a). The Douglas Creek Member intervals sampled are $\sim$300 m (CW1 core) and $\sim$400 m (M16 core) below the Curly tuff (Tuttle and Goldhaber, 1993). With estimated sedimentation rates ranging from 100 to 400 mm/Kyr in the Green River basins (Smith et al., 2008a), 400 m of sediment could have been deposited in 1 to 4 Myr. This suggests that the Re–Os dates for the Douglas Creek Member and the Mahogany Zone (Fig. 4) are in agreement with the Ar–Ar date for the Curly tuff (Fig. 2). A larger sequence stratigraphic study of the Uinta Basin would be needed to clarify this further. The oldest dated tuff in the adjacent Piceance Creek Basin is the Yellow tuff dated at 51.55 ± 0.52 Ma, which is stratigraphically equivalent to the lowest Douglas Creek Member and therefore should be and is older than the Re–Os dated sections. This agreement between the Ar–Ar and Re–Os geochronology demonstrates that the Re–Os system can be successfully applied to lacustrine organic-rich rocks to provide much-needed direct depositional age constraints in lacustrine basins, especially in the absence of Ar–Ar and U–Pb tuff geochronology. The concordance between direct and indirect depositional age determinations emphasises the expediency of geochronological methods for correlating global phenomena.

5.3. Re-Os uptake and fractionation

Our current understanding of the definitive controls of Re and Os uptake and fractionation in organic-rich rocks is incomplete. Here we briefly summarise previous findings and reveal how this study contributes to solving the dilemma emphasising the complex nature of Re and Os systematics in organic-rich rocks. Early studies suggested that sub-oxic to anoxic or euxinic conditions must exist for Re and Os uptake into organic-rich rocks, which occurs at or below the sediment–water interface (Cohen et al., 1999; Colodner et al., 1993; Crusius et al., 1996; Koide et al., 1991; Morford and Emerson, 1999). These studies and further experimental works provided evidence that Re and Os behave differently in the water column, with distinct uptake mechanisms and unknown controls on fractionation (Levasseur et al., 1998; Morford et al., 2009; Selby et al., 2009; Sundby et al., 2004; Yamashita et al., 2007). Recent work has also questioned the notion that Re and Os are directly linked to TOC values, with correlations occasionally but not always apparent despite the majority of these metals being held within the kerogen (Cohen et al., 1999; Rooney et al., 2012; Selby et al., 2009). High TOC requires high primary productivity with preservation potential reliant on a calm, oxygen-poor water body, without scavenging benthic life (Demaison and Moore, 1980; Sageman et al., 2003), however, these factors may not solely regulate Re and Os uptake and fractionation. Slow sedimentation has been proposed as one of the key factors in enhanced Re and Os uptake as seen for Ni and *V* enrichment in organic-rich rocks (Crusius and Thomson, 2000; Lewan and Maynard, 1982; Rooney et al., 2012; Selby et al., 2009). However, slow sedimentation may adversely affect TOC preservation due to the longer residence time for oxidation (Ibach, 1982). Aside from the principal condition requiring Re and Os in the water column, other influences that have been proposed to control Re and Os enrichment and fractionation are salinity (Martin et al., 2001), post-deposition mobility of the elements (Crusius and Thomson, 2000; Kendall et al., 2009a), pH and temperature (Georgiev et al., 2011). Since Re and Os are bound within the kerogen of an organic-rich rock (Rooney et al., 2012), but enrichment is affected by numerous processes beyond TOC preservation, a better appreciation of the organic matter chelating precursors of Re and Os is needed. In V and Ni studies it has been shown that the chelating precursor is not always preserved proportionally to organic matter (Lewan and Maynard, 1982) thus understanding the chelating precursor systematics of Re and Os will significantly advance our understanding of the Re–Os system.

Our data have shown that Re–Os geochronology can be successfully applied to lacustrine organic-rich rocks, and that element fractionation and abundances are similar to marine systems. However, the results are mixed with an accurate and precise isochron for the Douglas Creek Member (M16), but larger age uncertainties for the Mahogany Zone and Douglas Creek Member (CW1). We suggest that homogenous Re–Os fractionation is the cause of the larger uncertainty in the Mahogany Zone geochronology, although the reasons for this are currently ambiguous. In order to explain why these units behave differently in terms of Re–Os fractionation, TOC and Rock-Eval data are evaluated. These data yield insights into the GRF organic matter and hence Re–Os uptake and fractionation in lacustrine settings.

5.3.1. Insights from TOC and depositional conditions

In the three GRF units a positive but weak linear correlation of Re and common Os (^{192}Os) to TOC exists (Fig. 5A and B), with the Mahogany Zone displaying the best correlation. Rhenium versus TOC in the Mahogany Zone displays a positive trend (R^2 of 0.73)

yet the Douglas Creek Member shows no correlation (R^2 of 0.12 [CW1] and 0.17 [M16]). In terms of ^{192}Os versus TOC there is no strong correlation in any of the sections and they all have similar R^2 values (Mahogany Zone=0.56; Douglas Creek Member CW1=0.52; Douglas Creek Member M16=0.41). Despite weak correlations, the sampled horizons display variable relationships to TOC. The Douglas Creek Member (M16) has negligible correlation of both Re and Os to TOC, but much higher slopes than the other two units. These findings suggest an uptake mechanism possibly unrelated to TOC dominated in this region of the lake/water column, in contrast to Re and Os uptake in the Mahogany Zone which has the best correlation with TOC. The Douglas Creek Member represents a proximal lake margin setting during a time of fluctuating lake-levels producing variation in the sedimentation rate and terrigenous input; possibly allowing variable Re–Os uptake and fractionation. In contrast, the Mahogany Zone was deposited in the distal lake centre when lake-levels were at their maximum and enhanced primary productivity and slow and steady sedimentation rates in a stratified water column produced an extremely organic-rich and homogenous section (Boyer, 1982; Bradley, 1931; Smith et al., 2008a; Tuttle and Goldhaber, 1993). The homogenous depositional system of the Mahogany Zone may have allowed greater association of Re and Os with organic matter allowing less ^{187}Re/^{188}Os fractionation making precise Re–Os geochronology challenging. The relationship to depositional conditions suggests that, contrary to the Mahogany Zone, in the Douglas Creek Member sections the organic chelating components responsible for Re and Os uptake are not being preserved uniformly or that there are variable chelating surfaces derived from different organic matter types.

Additional GRF depositional factors to take into account are salinity, carbonate content and redox conditions. The Mahogany Zone is more saline and carbonate-rich than the Douglas Creek Member (Keighley et al., 2003; Tuttle and Goldhaber, 1993), with increased salinity creating greater water column stability and higher pH (Tuttle and Goldhaber, 1993). Improved water column stability may have been a contributing factor to the uniform preservation and Re–Os fractionation of the Mahogany Zone, however, these parameters cannot be fully assessed as there is no study of our samples quantifying salinity or carbonate content. Redox conditions of the GRF have not been directly studied although it has been suggested to be euxinic based on sulphur geochemistry (Tuttle and Goldhaber, 1993). During the late lake stage when the Mahogany Zone was deposited, δ^{34}S of sulphides (30–40‰) were higher than during deposition of the early stage Douglas Creek Member (δ^{34}S: 5–15‰). In particular the Mahogany Zone values are unusual as they are much higher than those in marine, freshwater or modern saline lake systems, reflecting complex sulphur geochemistry (Tuttle and Goldhaber, 1993). Fundamentally, the δ^{34}S values are due to a constant supply of sulphate to the lake being progressively reduced by sulphate reducing bacteria causing a gradual enrichment of ^{34}S. Euxinic systems have been previously dated using Re–Os geochronology with success (e.g., Kendall et al., 2009b), however the influence on Re–Os fractionation of extensive sulphate reduction and an abundance of H_2S are unknown. We suspect that the resulting stable water column stratification, particularly evident during Mahogany Zone deposition, is likely to have contributed to the homogenous Re–Os fractionation observed in the Mahogany Zone. This gives further indication of the complex nature of the controls on Re and Os uptake and fractionation and suggests that the depositional system plays a large role in the Re–Os organic system.

5.3.2. Effects of organic matter type

The relationship of Re and Os to TOC and depositional setting highlights that organic matter type may play a key role in Re and Os uptake and fractionation and so hydrogen index (HI) and oxygen index (OI) values from Rock-Eval pyrolysis are used to assess organic matter type of the GRF. A plot of HI/OI values indicates that all samples contain Type I kerogen, consistent with a lacustrine algal source of organic matter, with minimal terrestrial organic matter input (Fig. 3). The variation in HI and OI values cannot easily be explained by changing maturity as all the samples have similar T_{max} values (Peters, 1986; Table 1). Generally both the Douglas Creek Member horizons display more variability in both HI and OI than the Mahogany Zone (See inset Fig. 3). This is consistent with previous observations that strata from the central lake (e.g. Mahogany Zone) contain predominantly alganite organic matter, whereas samples deposited nearer the lake margins or during fluctuating lake-levels (e.g. Douglas Creek Member) contain alganite but also some vitrinite (Castle, 1990). The predominance of alganite in the Mahogany Zone coupled with the lack of Re-Os fractionation may suggest that organic matter type is a controlling factor in Re-Os fractionation. It has previously been postulated that Re and Os are bound by different organic ligands causing variable ^{187}Re/^{188}Os in different organic fractions (Miller, 2004), and also that an unknown method of biological uptake of Re over Os may occur (Georgiev et al., 2011). Our findings suggest that variation in organic matter type (e.g. from terrestrial and algal sources) may enable variable ^{187}Re/^{188}Os (as is seen in the Douglas Creek Member sections), whereas homogenous algal organic matter may lead to homogenous ^{187}Re/^{188}Os (as is seen in the Mahogany Zone) through providing uniform chelating sites for both elements. These findings have strong implications for any future Re-Os geochronological study, however, further studies are required to fully quantify and assess the relationship of Re and Os with organic matter.

Oxygen index is a proxy measurement of oxygen content in kerogen, which can be derived from terrestrial organic matter or oxidation of organic matter (Peters, 1986). We see no correlation between OI and Re and Os abundance (Fig. 5C and D) but below an OI value of ~15 mg CO_2/g TOC, abundances of both Re and Os increase. This may suggest that Re and Os enrichment requires lower oxygen-bearing kerogen or lower oxygen conditions in which the kerogen was deposited. Vanadium and Ni have been found to be bound in tetrapyrroles, of which chlorophyll is the main precursor (Lewan and Maynard, 1982). Chlorophyll is sensitive to oxygen as it opens up the ring structure making it incapable of hosting metals and so sediments settling in an oxygenated water column will have less chance to bind *V* and Ni in tetrapyrroles (Lewan and Maynard, 1982). The binding sites of Re and Os are unknown, but the relationship with OI illustrates the importance of deducing where these metals are held. If Re and Os are more enriched at low OI, this suggests that oxygen has a significant effect on the chelating precursors of Re and Os during deposition and also that the chelating precursors of Re and Os cannot be related to carboxyl complexes. The OI also seems to exert a minor control on ^{187}Re/^{188}Os fractionation below 15 mg CO_2/g TOC (Fig. 5E). This would support the findings of Yamashita et al. (2007) who note that Re is more readily incorporated into organic-rich rocks under highly reducing conditions leading to high ^{187}Re/^{188}Os. However, this study and previous studies concluded that specific controls on fractionation are poorly constrained. For organic matter of lacustrine sedimentary rocks, the non-linear relationship between OI and Re and Os potentially suggests that oxygen content in kerogen and/or organic matter type have a significant effect on chelation of Re and Os and hence Re-Os fractionation. If this proves to be the case in other studied sections, OI may provide a means of assessing whether a section

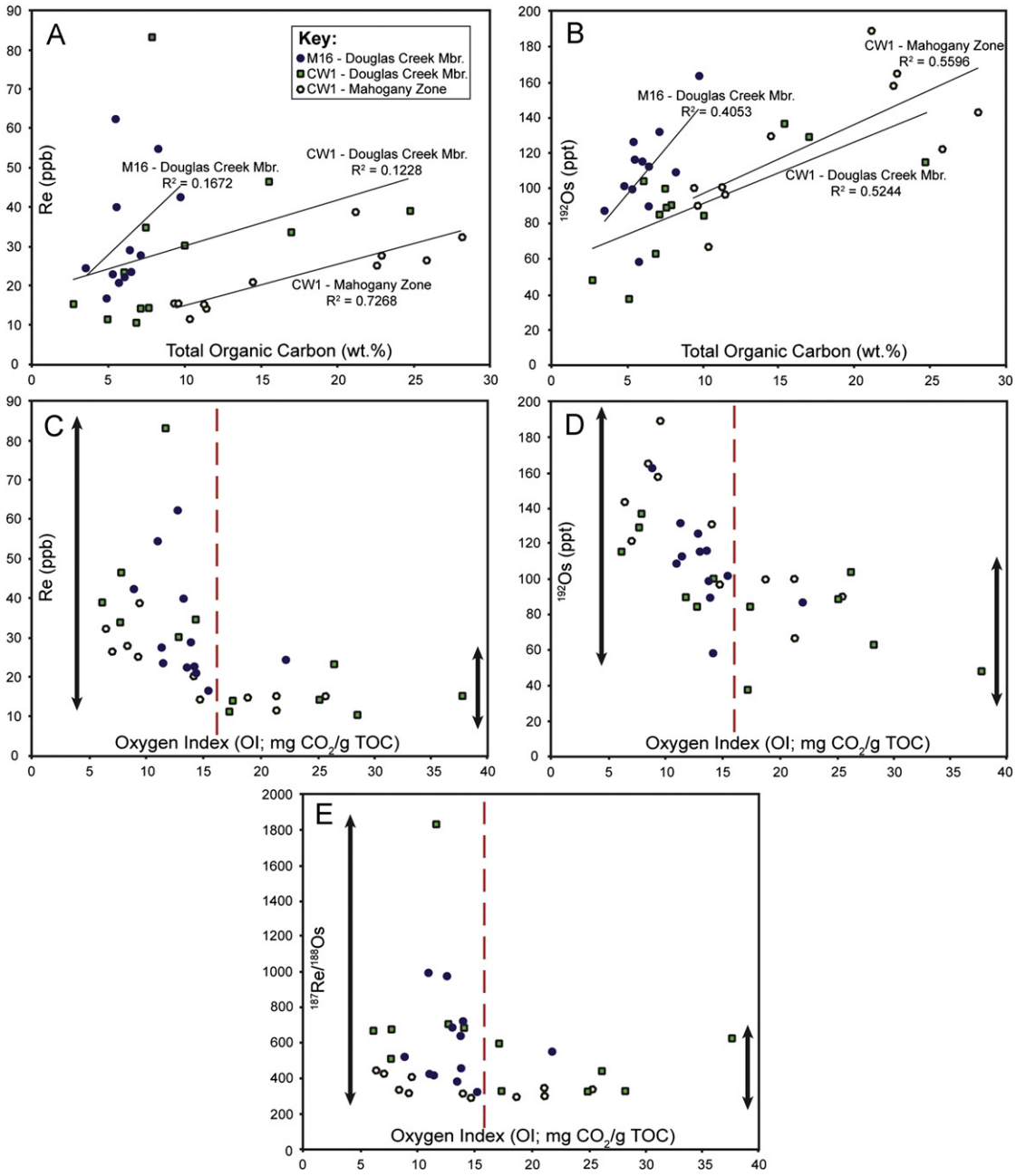

Fig. 5. Graphs of total organic carbon (TOC) versus Re (A) and ^{192}Os (B) of all the studied Green River Formation units showing linear correlations. Common Os (^{192}Os) is plotted to remove the effect of radiogenic in-growth. R^2 for each unit is annotated on the graphs. Oxygen index (OI) versus Re (C), ^{192}Os (D) and ^{187}Re/^{188}Os (E) of all the units are also plotted. The dashed line represents the threshold OI below which Re and Os concentrations are increased, and ^{187}Re/^{188}Os values are more variable (see text for discussion). The black bars represent the amount of variation in Re, Os and ^{187}Re/^{188}Os on each side of the dashed threshold line.

may be viable for precise Re-Os geochronology providing an understanding of maturity and organic matter variation exists as these can affect OI values. However, as OI is a proxy for the atomic O/C ratio, future studies of atomic O/C versus Re–Os may shed further light on these findings and on the chelating precursors of Re and Os. Previous work has utilised OI as a proxy for weathering in order to assess Re–Os isochroneity, with non-isochronous samples possessing higher OI suggested to be caused by weathering (Georgiev et al., 2012). Disparity in OI can be caused by organic facies and maturity variations and therefore can only be a proxy for weathering in a weathering profile of identical strata. As such, ranges in OI should not be employed as a tool for estimating weathering intensity of differing strata.

5.4. Os isotope systematics

The Re-Os isotope data yield Os_i values of 1.54 ± 0.03, 1.41 ± 0.06 and 1.48 ± 0.06 (Fig. 4) for the M16 Douglas Creek Member, CW1 Douglas Creek Member, and CW1 Mahogany Zone, respectively, suggesting a radiogenic terrestrial source of Os in the Uinta lake water column, derived primarily from continental runoff. The variation in Os_i between the three units may be explained by the proximity to different Os sources (e.g., radiogenic Precambrian crust or unradiogenic volcanic units) and the temporal variation in weathering into the Uinta Lake water column. Spatial and temporal variations related to drainage variation are also observed in Sr isotope studies from the Uinta and Greater Green River Basins (Davis et al., 2008;

Rhodes et al., 2002). In the Uinta Basin Sr resolution through the GRF is low, but $^{87}Sr/^{86}Sr$ is radiogenic (mean: 0.71183) and fluctuates (Davis et al., 2008) similarly to the Os_i from this study. In the Greater Green River Basin Sr exhibits fluctuations with more radiogenic $^{87}Sr/^{86}Sr$ (up to 0.71331) during lowstands due to more exposure of radiogenic crust leading to increased riverine input of radiogenic Sr (Rhodes et al., 2002). Although Sr and Os records are decoupled, we suggest that this may also be a contributing factor to the change in Os_i seen in the separate samples used for Re-Os geochronology (see Fig. 4 insets and Table 1), although higher resolution Os isotope stratigraphy through the GRF would be needed to confirm this. In light of the results from this study it is clear that the Os_i of lacustrine sediments, like Sr, can be a useful tool for deducing continental geological processes as it responds to changes in drainage from the surrounding geology, in turn controlled by regional climate, tectonics and magmatism. Oceanic Os has a shorter residence time ($\leq$10,000 years) than Sr (1–4 Myrs), thus yielding much higher resolution perturbations in the geochemical record (Peucker-Ehrenbrink and Ravizza, 2000). However, the variable geological history of lakes means that each lake would need to be assessed individually to deduce Os and Sr residence time.

In addition to providing information about the regional geology and climate, the Os_i can also provide high-resolution data are able to distinguish between marine and lacustrine deposition where other methods fail. The depositional setting of sedimentary basins is often ambiguous and can transition from lacustrine to marine to restricted marine with few clues to the precise nature and timing of these events. An Os isotope stratigraphic study of Lomonosov Ridge sediments from the Arctic Ocean revealed a change from 'lake stage' deposition to oceanic conditions (Poirier and Hillaire-Marcel, 2011). In this case the Os_i is radiogenic (up to 1.3) during the 'lake stage' and with a change to oceanic conditions, the Os_i ($\sim$0.4) then matches the Cenozoic seawater $^{187}Os/^{188}Os$ curve. This allows for the exact transition in the stratigraphy to be determined. Poirier and Hillaire-Marcel's (2011) study coupled with data from this study suggest that if the $^{187}Os/^{188}Os$ of seawater at the time of sediment deposition is known (e.g., seawater during GRF deposition = $\sim$0.56; Kato et al., 2011), large deviations from this value would suggest that the sediments are not marine. Therefore Os_i stratigraphy could be especially helpful in basins where the depositional origin is uncertain or in marine basins that have undergone periods of restriction for unknown lengths of time.

Reconstructing the global ocean Os isotope record and understanding its fluctuations is a major challenge for our understanding of ocean chemistry (Peucker-Ehrenbrink and Ravizza, 2012, 2000). During the Cenozoic, the global ocean Os isotope composition became progressively more radiogenic (0.56 at 50 Ma to a modern day ratio of 1.06; Kato et al., 2011; Peucker-Ehrenbrink and Ravizza, 2000). The specific causes behind this change in Os isotope composition are unknown although similar changes in the Sr record have been related to increases in continental weathering due, principally, to the uplift of the Himalayas (Raymo and Ruddiman, 1992; Richter et al., 1992). However, these two records are decoupled as they vary in their influences and respective residence times and it has also been suggested that the Himalayas are not the dominant source of Os to the oceans during the Cenozoic (Sharma et al., 1999). An underlying problem is that, while we can reconstruct the past global ocean Os curve, we cannot accurately deduce the nature and changes in the sources of Os to the ocean and therefore cannot make accurate inferences as to what is causing the perturbations. Gaining further understanding of the sources of Os to the ocean in the past is vital to further elucidate these problems. The only reliable records of the geochemical composition of past continental runoff are lacustrine sediments as they are minimally affected by other potential inputs into the oceans (e.g. cosmic dust, mid-ocean ridge hydrothermal alteration). In this study the Os_i of the GRF (1.41–1.54) provides the $^{187}Os/^{188}Os$ composition of regional continental runoff into the Green River lakes, similar to estimates for present day $^{187}Os/^{188}Os$ composition of upper continental crust (1.40; Peucker-Ehrenbrink and Ravizza, 2000) and continental runoff (1.54; Levasseur et al., 1999). This similarity may suggest that the composition of continental runoff in the Eocene may have been comparable to the present day. While the GRF Os_i cannot be used as a sole representation of continental runoff into the ocean, it can be noted that lacustrine basins do give an insight into past continental runoff regimes. Though this study cannot rule out radiogenic flux of Os from weathering as the cause of the increase in seawater $^{187}Os/^{188}Os$ over the last 50 Ma, it highlights that continental runoff may not have been the driving force for these changes. Variations in the unradiogenic input to the oceans between 50 Ma and the present day should be more closely examined as a potential cause for seawater $^{187}Os/^{188}Os$ changes. Poirier and Hillaire-Marcel (2011) also find radiogenic $^{187}Os/^{188}Os$ (up to 1.3 at $\sim$36 Ma) during the Arctic Ocean's 'lake stage' before it became fully connected with the global ocean. They suggest that the opening of the Fram Strait may have swamped the global ocean with radiogenic Os contributing to the Cenozoic seawater increase in $^{187}Os/^{188}Os$. These Os isotope studies of lacustrine systems provide valuable insights into continental Os inputs to the oceans and with further research could be used to reconstruct a picture of past global continental runoff and its influence on climate change.

6. Conclusions

The Re–Os systematics of three core intervals of the GRF yield dates that are in agreement, within uncertainty, of U–Pb and Ar–Ar tuff geochronology. This demonstrates that the Re–Os geochronometer can be successfully applied to lacustrine carbonaceous organic-rich rocks, providing a valuable tool for determining the direct depositional history of lacustrine systems and furthermore, for understanding and correlating continental geological processes. Coupled with previous Re–Os studies, our data suggest that, in general, any rock type deposited in conditions where organic matter is preserved is viable for Re–Os geochronology and the tool is not restricted to marine black shales, making this a far-reaching tool for lacustrine and marine depositional settings alike.

This study brings further to light the complexity of Re–Os systematics in organic-rich rocks. The Re–Os dates for the Douglas Creek Member are controlled by the degree of variability of the initial $^{187}Os/^{188}Os$ composition within the sampled 2 m interval. For the Mahogany Zone the imprecise age relates to a small spread in $^{187}Re/^{188}Os$ values comparable to those seen in some marine systems (Turgeon et al., 2007). We suggest that the controls on Re and Os fractionation within organic-rich rocks are complex but in this case are related to depositional environment (proximal lake shore versus distal lake centre) and organic matter type (terrestrial versus algal). The relationship of Re and Os to OI highlights the importance of understanding the chelating precursors of Re and Os in organic matter, in order to further our knowledge of the Re–Os organic-rich sediment geochronometer.

In addition to geochronology, the initial $^{187}Os/^{188}Os$ composition of lacustrine organic-rich rocks can be used to determine the geochemical signature of continental runoff into lake basins. This yields a potential tool to distinguish between marine and lacustrine sediments when seawater $^{187}Os/^{188}Os$ is well

characterised (this study; Poirier and Hillaire-Marcel, 2011). Furthermore, Os isotope stratigraphy of lacustrine successions can be applied to understanding regional climatic, tectonic and magmatic regimes and allows for chemostratigraphic correlations that combine direct depositional ages, giving much higher confidence in global correlations.

Acknowledgements

This research was funded by a Lundin Petroleum CeREES PhD scholarship and the Rocky Mountain Association of Geologists Norman H. Foster scholarship awarded to VMC. The USGS Core Research Centre is thanked for provision of samples and help with sample collection. Michelle Tuttle is thanked for help with core logs and sample information. Mark Allen, Dick Keefer, Greg Ravizza, Mike Lewan and Brian Marshall are thanked for valuable contributions to previous versions of this manuscript. Katz Suzuki and an anonymous reviewer are thanked for helpful reviews of the manuscript. Any use of trade, firm, or product names is for descriptive purposes only and does not imply endorsement by the U.S. Government.

Appendix A. Supporting information

Supplementary data associated with this article can be found in the online version at http://dx.doi.org/10.1016/j.epsl.2012.10.012.

References

Baioumy, H.M., Eglinton, L.B., Peucker-Ehrenbrink, B., 2011. Rhenium–osmium isotope and platinum group element systematics of marine vs. non-marine organic-rich sediments and coals from Egypt. Chem. Geol. 285, 70–81.

Boyer, B.W., 1982. Green River laminites: does the playa-lake model really invalidate the stratified-lake model? Geology 10, 321–324.

Bradley, W.H., 1931. Origin and microfossils of the oil shale of the Green River Formation of Colorado and Utah. US Geological Survey, Professional paper 168.

Carroll, A.R., Bohacs, K.M., 2001. Lake-type controls on petroleum source rock potential in nonmarine basins. AAPG Bull. 85, 1033–1053.

Carroll, A.R., Bohacs, K.M., 1999. Stratigraphic classification of ancient lakes: balancing tectonic and climatic controls. Geology 27, 99–102.

Carroll, A.R., Brassell, S.C., Graham, S.A., 1992. Upper Permian lacustrine oil shales, southern Junggar Basin, Northwest China. AAPG Bull. 76, 1874–1902.

Castle, J.W., 1990. Sedimentation in Eocene lake Uinta (Lower Green River Formation), northeastern Uinta basin, Utah. in: Katz, B.J. (Ed.), Lacustrine Basin Exploration: Case Studies and Modern Analogs, AAPG Memoir 50, AAPG Tulsa, pp. 243–263.

Cohen, A.S., Coe, A.L., Bartlett, J.M., Hawkesworth, C.J., 1999. Precise Re–Os ages of organic-rich mudrocks and the Os isotope composition of Jurassic seawater. Earth Planet. Sci. Lett. 167, 159–173.

Colodner, D., Sachs, J., Ravizza, G., Turekian, K., Edmond, J., Boyle, E., 1993. The geochemical cycles of rhenium: a reconnaissance. Earth Planet. Sci. Lett. 117, 205–221.

Creaser, R., Szatmari, P., Milani, E.J., 2008. Extending Re–Os shale geochronology to lacustrine depositional systems: a case study from the major hydrocarbon source rocks of the Brazilian Mesozoic marginal basins. In: Proceedings of the 33rd International Geological Congress, Oslo (abstract).

Creaser, R.A., Sannigrahi, P., Chacko, T., Selby, D., 2002. Further evaluation of the Re–Os geochronometer in organic-rich sedimentary rocks: a test of hydrocarbon maturation effects in the Exshaw Formation, Western Canada Sedimentary Basin. Geochim. Cosmochim. Acta 66, 3441–3452.

Crusius, J., Calvert, S., Pedersen, T., Sage, D., 1996. Rhenium and molybdenum enrichments in sediments as indicators of oxic, suboxic and sulfidic conditions of deposition. Earth Planet. Sci. Lett. 145, 65–78.

Crusius, J., Thomson, J., 2000. Comparative behavior of authigenic Re, U, and Mo during reoxidation and subsequent long-term burial in marine sediments. Geochim. Cosmochim. Acta 64, 2233–2242.

Davis, S.J., Wiegand, B.A., Carroll, A.R., Chamberlain, C.P., 2008. The effect of drainage reorganization on paleoaltimetry studies: an example from the Paleogene Laramide foreland. Earth Planet. Sci. Lett. 275, 258–268.

Demaison, G.J., Moore, G.T., 1980. Anoxic environments and oil source bed genesis. Org. Geochem. 2, 9–31.

Dyni, J.R., 2006. Geology and resources of some world oil-shale deposits. US Geological Survey Scientific Investigations Report 2005, 5294.

Espitalie, J., Laporte, J.L., Madec, M., Marquis, F., Leplat, P., Paulet, J., Boutefeu, A., 1977. Rapid method for source rocks characterization and for determination of petroleum potential and degree of evolution. Rev. Inst. Fr. Pet. Ann. 32, 23–42.

Esser, B.K., Turekian, K.K., 1993. The osmium isotopic composition of the continental-crust. Geochim. Cosmochim. Acta 57, 3093–3104.

Georgiev, S., Stein, H.J., Hannah, J.L., Bingen, B., Weiss, H.M., Piasecki, S., 2011. Hot acidic late Permian seas stifle life in record time. Earth Planet. Sci. Lett. 310, 389–400.

Georgiev, S., Stein, H.J., Hannah, J.L., Weiss, H.M., Bingen, B., Xu, G., Rein, E., Hatløy, V., Løseth, H., Nali, M., Piasecki, S., 2012. Chemical signals for oxidative weathering predict Re–Os isochroneity in black shales, East Greenland. Chem. Geol. 324–325, 108–121.

Hao, F., Zhou, X., Zhu, Y., Yang, Y., 2011. Lacustrine source rock deposition in response to co-evolution of environments and organisms controlled by tectonic subsidence and climate, Bohai Bay Basin, China. Org. Geochem. 42, 323–339.

Hattori, Y., Suzuki, K., Honda, M., Shimizu, H., 2003. Re–Os isotope systematics of the Taklimakan Desert sands, moraines and river sediments around the Taklimakan Desert, and of Tibetan soils. Geochim. Cosmochim. Acta 67, 1203–1213.

Hunt, J.M., 1996. Petroleum Geochemistry and Geology, 2nd ed. W.H. Freeman and Company, New York.

Ibach, L.E.J., 1982. Relationship between sedimentation-rate and total organic carbon content in ancient marine-sediments. AAPG Bull. Am. Assoc. Pet. Geol. 66, 170–188.

Johnson, J.G., Klapper, G., Sandberg, C.A., 1985. Devonian eustatic fluctuations in Euramerica. Geol. Soc. Am. Bull. 96, 567–587.

Johnson, S.Y., 1992. Phanerozoic evolution of sedimentary basins in the Uinta–Piceance Basin region, northwestern Colorado and northeastern Utah. US Geological Survey Bulletin 1787-FF.

Kato, Y., Fujinaga, K., Suzuki, K., 2011. Marine Os isotopic fluctuations in the early Eocene greenhouse interval as recorded by metalliferous umbers from a Tertiary ophiolite in Japan. Gondwana Res. 20, 594–607.

Katz, B.J., 2001. Lacustrine basin hydrocarbon exploration – current thoughts. J. Paleolimnol. 26, 161–179.

Katz, B.J., 1995. The Green River Shale: an Eocene Carbonate Lacustrine Source Rock. in: Katz, B.J. (Ed.), Petroleum Source Rocks. Springer-Verlag, Berlin, Heidelberg, pp. 309–324.

Keighley, D., Flint, S., Howell, J., Moscariello, A., 2003. Sequence stratigraphy in lacustrine basins: a model for part of the Green River Formation (Eocene), Southwest Uinta Basin, Utah, USA. J. Sediment. Res. 73, 987–1006.

Kendall, B., Creaser, R.A., Selby, D., 2009a. ^{187}Re–^{187}Os geochronology of Precambrian organic-rich sedimentary rocks. Geological Society, 326. Special Publications, London, pp. 85–107.

Kendall, B., Creaser, R.A., Gordon, G.W., Anbar, A.D., 2009b. Re–Os and Mo isotope systematics of black shales from the Middle Proterozoic Velkerri and Wollogorang formations, McArthur Basin, northern Australia. Geochim. Cosmochim. Acta 73, 2534–2558.

Kendall, B.S., Creaser, R.A., Ross, G.M., Selby, D., 2004. Constraints on the timing of Marinoan "Snowball Earth" glaciation by ^{187}Re–^{187}Os dating of a Neoproterozoic, post-glacial black shale in Western Canada. Earth Planet. Sci. Lett. 222, 729–740.

Koide, M., Goldberg, E.D., Niemeyer, S., Gerlach, D., Hodge, V., Bertine, K.K., Padova, A., 1991. Osmium in marine sediments. Geochim. Cosmochim. Acta 55, 1641–1648.

Kuiper, K.F., Deino, A., Hilgen, F.J., Krijgsman, W., Renne, P.R., Wijbrans, J.R., 2008. Synchronizing rock clocks of Earth history. Science 320, 500–504.

Lambiase, J.J., 1990. A model for tectonic control of lacustrine stratigraphic sequences in continental rift basins. in: Katz, B.J. (Ed.), Lacustrine Basin Exploration: Case Studies and Modern Analogs. AAPG Memoir 50, AAPG Tulsa, pp. 265–276.

Levasseur, S., Birck, J., Allegre, C.J., 1998. Direct measurement of femtomoles of osmium and the $^{187}Os/^{186}Os$ ratio in seawater. Science 282, 272–274.

Levasseur, S., Birck, J.L., Allègre, C.J., 1999. The osmium riverine flux and the oceanic mass balance of osmium. Earth Planet. Sci. Lett. 174, 7–23.

Lewan, M.D., Maynard, J.B., 1982. Factors controlling enrichment of vanadium and nickel in the bitumen of organic sedimentary rocks. Geochim. Cosmochim. Acta 46, 2547–2560.

Ludwig, K., 2008. Isoplot, version 4.0: a geochronological toolkit for microsoft Excel. Berkeley Geochronology Centre Special Publication no. 4.

Ludwig, K.R., 1980. Calculation of uncertainties of U-Pb isotope data. Earth Planet. Sci. Lett. 46, 212–220.

Machlus, M., Hemming, S.R., Olsen, P.E., Christie-Blick, N., 2004. Eocene calibration of geomagnetic polarity time scale reevaluated: evidence from the Green River Formation of Wyoming. Geology 32 (137–140).

Martin, C.E., Peucker-Ehrenbrink, B., Brunskill, G., Szymczak, R., 2001. Osmium isotope geochemistry of a tropical estuary. Geochim. Cosmochim. Acta 65, 3193–3200.

McArthur, J.M., Algeo, T.J., van de Schootbrugge, B., Li, Q., Howarth, R.J., 2008. Basinal restriction, black shales, Re–Os dating, and the Early Toarcian (Jurassic) oceanic anoxic event. Paleoceanography 23 (4), PA4217.

Meyers, S.R., 2008. Resolving Milankovitchian controversies: the Triassic Latemar Limestone and the Eocene Green River Formation. Geology 36, 319–322.

Miller, C.A., 2004. Re–Os dating of algal laminites: reduction-enrichment of metals in the sedimentary environment and evidence for new geoporphyrins. Masters Thesis, University of Saskatchewan, pp. 124–128.
Morford, J.L., Emerson, S., 1999. The geochemistry of redox sensitive trace metals in sediments. Geochim. Cosmochim. Acta 63, 1735–1750.
Morford, J.L., Martin, W.R., Francois, R., Carney, C.M., 2009. A model for uranium, rhenium, and molybdenum diagenesis in marine sediments based on results from coastal locations. Geochim. Cosmochim. Acta 73, 2938–2960.
Olsen, P.E., 1997. Stratigraphic record of the early Mesozoic breakup of Pangea in the Laurasia–Gondwana rift system. Annu. Rev. Earth Planet. Sci. 25, 337–401.
Peters, K.E., 1986. Guidelines for evaluating petroleum source rock using programmed pyrolysis. AAPG Bull. 70, 318–329.
Peucker-Ehrenbrink, B., Jahn, B.-m., 2001. Rhenium–osmium isotope systematics and platinum group element concentrations: Loess and the upper continental crust. Geochem. Geophys. Geosyst. 2 (10), 1061–1083.
Peucker-Ehrenbrink, B., Ravizza, G., 2012. Osmium isotope stratigraphy. in: Gradstein, F.M., Ogg, J.G., Schmitz, M., Ogg, G. (Eds.), The Geological Timescale, 1. Elsevier, Oxford, pp. 145–166.
Peucker-Ehrenbrink, B., Ravizza, G., 2000. The marine osmium isotope record. Terr. Nova 12, 205–219.
Pietras, J.T., Carroll, A.R., 2006. High-resolution stratigraphy of an underfilled lake Basin: Wilkins Peak Member, Eocene Green River Formation, Wyoming, USA. J. Sediment. Res. 76, 1197–1214.
Poirier, A., Hillaire-Marcel, C., 2011. Improved Os-isotope stratigraphy of the Arctic Ocean. Geophys. Res. Lett. 38, L14607.
Ravizza, G., Turekian, K.K., 1992. The osmium isotopic composition of organic-rich marine sediments. Earth Planet. Sci. Lett. 110, 1–6.
Ravizza, G., Turekian, G.G., Hay, B.J., 1991. The geochemistry of rhenium and osmium in recent sediments from the Black Sea. Geochim. Cosmochim. Acta 55, 3741–3752.
Ravizza, G., Turekian, K.K., 1989. Application of the ^{187}Re-^{187}Os system to black shale geochronometry. Geochim. Cosmochim. Acta 53, 3257–3262.
Raymo, M.E., Ruddiman, W.F., 1992. Tectonic forcing of late Cenozoic climate. Nature 359, 117–122.
Remy, R.R., 1992. Stratigraphy of the Eocene part of the Green River Formation in the South-Central Part of the Uinta Basin, Utah. US Geological Survey Bulletin 1787-BB.
Rhodes, M.K., Carroll, A.R., Pietras, J.T., Beard, B.L., Johnson, C.M., 2002. Strontium isotope record of paleohydrology and continental weathering, Eocene Green River Formation, Wyoming. Geology 30, 167–170.
Richter, F.M., Rowley, D.B., Depaolo, D.J., 1992. Sr isotope evolution of seawater – the role of tectonics. Earth Planet. Sci. Lett. 109, 11–23.
Rooney, A.D., Selby, D., Houzay, J.-P., Renne, P.R., 2010. Re–Os geochronology of a Mesoproterozoic sedimentary succession, Taoudeni basin, Mauritania: implications for basin-wide correlations and Re–Os organic-rich sediments systematics. Earth Planet. Sci. Lett. 289, 486–496.
Rooney, A.D., Selby, D., Lewan, M.D., Lillis, P.G., Houzay, J.-P., 2012. Evaluating Re–Os systematics in organic-rich sedimentary rocks in response to petroleum generation using hydrous pyrolysis experiments. Geochim. Cosmochim. Acta 77, 275–291.
Ruble, T.E., Lewan, M.D., Philp, R.P., 2001. New insights on the Green River Petroleum System in the Uinta Basin from hydrous pyrolysis experiments. AAPG Bull. 85, 1333–1371.
Ryder, R.T., Fouch, T.D., Elison, J.H., 1976. Early Tertiary sedimentation in the Western Unita Basin, Utah. Geol. Soc. Am. Bull. 87, 496–512.
Sageman, B.B., Murphy, A.E., Werne, J.P., Ver Straeten, C.A., Hollander, D.J., Lyons, T.W., 2003. A tale of shales: the relative roles of production, decomposition, and dilution in the accumulation of organic-rich strata, middle–upper Devonian, Appalachian basin. Chem. Geol. 195, 229–273.
Selby, D., 2007. Direct rhenium–osmium age of the Oxfordian–Kimmeridgian boundary, Staffin bay, Isle of Skye, UK, and the late Jurassic time scale. Norw. J. Geol. 87, 291–300.
Selby, D., Creaser, R.A., 2003. Re–Os geochronology of organic rich sediments: an evaluation of organic matter analysis methods. Chem. Geol. 200, 225–240.
Selby, D., Creaser, R.A., 2005. Direct radiometric dating of the Devonian–Mississippian time-scale boundary using the Re–Os black shale geochronometer. Geology 33, 545–548.
Selby, D., Creaser, R.A., Stein, H.J., Markey, R.J., Hannah, J.L., 2007. Assessment of the Re-187 decay constant by cross calibration of Re–Os molybdenite and U–Pb zircon chronometers in magmatic ore systems. Geochim. Cosmochim. Acta 71, 1999–2013.
Selby, D., Mutterlose, J., Condon, D.J., 2009. U–Pb and Re–Os geochronology of the Aptian/Albian and Cenomanian/Turonian stage boundaries: implications for timescale calibration, osmium isotope seawater composition and Re–Os systematics in organic-rich sediments. Chem. Geol. 265, 394–409.
Sharma, M., Wasserburg, G.J., Hofmann, A.W., Chakrapani, G.J., 1999. Himalayan uplift and osmium isotopes in oceans and rivers – its relation to global tectonics and climate. Geochim. Cosmochim. Acta 63, 4005–4012.
Smith, M.E., Carroll, A.R., Singer, B.S., 2008a. Synoptic reconstruction of a major ancient lake system: Eocene Green River Formation, western United States. Geol. Soc. Am. Bull. 120, 54–84.
Smith, M.E., Carroll, A.R., Mueller, E.R., 2008b. Elevated weathering rates in the rocky mountains during the early Eocene climatic optimum. Nat. Geosci. 1, 370–374.
Smith, M.E., Chamberlain, K.R., Singer, B.S., Carroll, A.R., 2010. Eocene clocks agree: Coeval ^{40}Ar/^{39}Ar, U–Pb, and astronomical ages from the Green River Formation. Geology 38, 527–530.
Smith, M.E., Singer, B., Carroll, A., 2003. ^{40}Ar/^{39}Ar geochronology of the Eocene Green River Formation, Wyoming. Geol. Soc. Am. Bull. 115, 549–565.
Smith, M.E., Singer, B.S., Carroll, A.R., Fournelle, J.H., 2006. High-resolution calibration of Eocene strata: ^{40}Ar/^{39}Ar geochronology of biotite in the Green River Formation. Geology 34, 393–396.
Smoliar, M.I., Walker, R.J., Morgan, J.W., 1996. Re–Os isotope constraints on the age of Group IIA, IIIA, IVA, and IVB iron meteorites. Science 271, 1099–1102.
Sun, W.D., Bennett, V.C., Eggins, S.M., Kamenetsky, V.S., Arculus, R.J., 2003. Enhanced mantle-to-crust rhenium transfer in undegassed arc magmas. Nature 422, 294–297.
Sundby, B., Martinez, P., Gobeil, C., 2004. Comparative geochemistry of cadmium, rhenium, uranium, and molybdenum in continental margin sediments. Geochim. Cosmochim. Acta 68, 2485–2493.
Tissot, B., Deroo, G., Hood, A., 1978. Geochemical study of the Uinta basin: formation of petroleum from the Green River Formation. Geochim. Cosmochim. Acta 42, 1469–1485.
Turgeon, S.C., Creaser, R.A., Algeo, T.J., 2007. Re–Os depositional ages and seawater Os estimates for the Frasnian–Famennian boundary: implications for weathering rates, land plant evolution, and extinction mechanisms. Earth Planet. Sci. Lett. 261, 649–661.
Tuttle, M.L., Goldhaber, M.B., 1993. Sedimentary sulfur geochemistry of the Paleogene Green River Formation, western USA: implications for interpreting depositional and diagenetic processes in saline alkaline lakes. Geochim. Cosmochim. Acta 57, 3023–3039.
Ver Straeten, C.A., Brett, C.E., Sageman, B.B., 2011. Mudrock sequence stratigraphy: a multi-proxy (sedimentological, paleobiological and geochemical) approach, Devonian Appalachian Basin. Palaeogeog. Palaeoclim. Palaeoecol. 304, 54–73.
Xu, G.P., Hannah, J.L., Stein, H.J., Bingen, B., Yang, G., Zimmerman, A., Weitschat, W., Mork, A., Weiss, H.M., 2009. Re–Os geochronology of Arctic black shales to evaluate the Anisian–Ladinian boundary and global faunal correlations. Earth Planet. Sci. Lett. 288, 581–587.
Yamashita, Y., Takahashi, Y., Haba, H., Enomoto, S., Shimizu, H., 2007. Comparison of reductive accumulation of Re and Os in seawater–sediment systems. Geochim. Cosmochim. Acta 71, 3458–3475.
Yang, G., Hannah, J.L., Zimmerman, A., Stein, H.J., Bekker, A., 2009. Re–Os depositional age for Archean carbonaceous slates from the southwestern superior province: challenges and insights. Earth Planet. Sci. Lett. 280, 83–92.